Journal of Power Sources, 2 (1977/78) 301 - 316

A SYSTEM EVALUATION OF LEAD–ACID BATTERY CHARGERS: PART I. CELLS WITH ANTIMONIAL POSITIVE GRIDS*

J. L. WEININGER and E. G. SIWEK

General Electric Company, Corporate Research and Development, P.O. Box 8, Schenectady, N.Y. 12301 (U.S.A.)

(Received April 27, 1977; in revised form July 27, 1977)

Summary

Three lead–acid battery charge control methods are evaluated on the basis of battery cycle life, changes in charging efficiency during successive cycling, and the effects of battery design on charger/battery interaction.

Lead–acid battery charging systems which use gases evolved from the battery during charge as a means for charging control are potentially more efficient than conventional battery charging systems. Further, it is expected that gas-controlled charging systems can result in prolonged life because they avoid elevated temperatures associated with overcharging and excessive gassing which loosen active materials from the plate structure during overcharge.

The selection of a suitable current profile is discussed, followed by a description of the three charging methods. Details are given for the two types of batteries tested, for the testing procedure, and the resulting battery performance throughout cycle life.

Zusammenfassung

Drei Ladekontrollmethoden für Säurebatterien werden ausgewertet unter Zugrundelegung der Lebensdauer der Batterien, der Unterschiede bei der Ladekapazität bei aufeinanderfolgenden Perioden und der Auswirkungen des Batterie–Modells auf die Wechselwirkung Ladegerät/Batterie.

Ladesysteme für Säurebatterien, die die von der Batterie beim Aufladen abgegebenen Gase als Ladekontrolle benutzen, sind möglicherweise sehr viel leistungsfähiger als herkömmliche Batterie–Ladesysteme. Ausserdem hofft man, dass gaskontrollierte Ladesysteme eine höhere Lebensdauer bewirken, da sie die mit einer Überladung in Zusammenhang stehenden erhöhten Temperaturen und übermässige Gasabgabe verhindern, durch die sich aktive Masse von der Plattenstruktur bei einer Überladung ablöst.

---

*Part II of this paper, Cells with cast lead–calcium grids, appears on pp. 317 - 336 of this issue of the journal.

Die Auswahl einer geeigneten Ladestromkurve wird diskutiert, woran sich eine Beschreibung der drei Lademethoden anschliesst. Einzelheiten zu den beiden untersuchten Batterietypen, zu dem Testverfahren und zu der daraus resultierenden Batterie-Leistung über die gesamte Lebensdauer sind angegeben.

Current Profile Selection

For this program, maximum charging efficiency was desired as well as maximum battery life. These two goals are consistent since an efficient charge, because of its minimal gassing and minimal temperature rise during charge, results in prolonged battery life.

The charging current–time profile which results in a charge of maximum efficiency is that which coincides with the battery charge acceptance curve. This is illustrated by the idealized charge acceptance curve of Fig. 1.

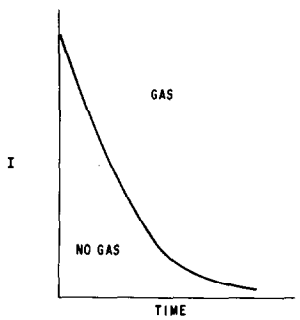

Fig. 1. Idealized charge acceptance curve.

The curve corresponds to a maximum acceptable initial charging current and a finishing current just sufficient to maintain the battery above its self-discharge rate. In the case of one of the 12 A h batteries tested (battery A below), these ideal values previously had been found to be 55 and 0.12 A. However, for practical purposes, because initial extremely high charging currents were too difficult to manage within the scope of this work, a 2 C initial charging rate (24 A) was used for the three charging modes under study. Similarly, the end of charge rate proved to be too small especially for aging batteries, so that a finishing rate of 0.24 to 0.48 A (C/50 to C/24) and higher was chosen in this work.

Charging Methods

Of the three selected charging modes, two were based on gas control, by either mass flow or differential pressure control. The third method was a

modified constant potential (MCP) method, which was chosen for comparison as a more conventional charging method. All three of these charging methods rely upon an exponentially decaying charging current, capable of reflecting and responding to the battery's diminishing charge acceptance during charging.

The conventional MCP charging method is the simplest of the three charging modes selected. For this type of charge, two parameters are selected: the initial charging current and the constant charging voltage. The term "modified", when applied to this charging method, indicates that the initial charging current has been limited so that large current spikes are avoided at the beginning of a charge, as would be the case at the beginning of charge of a fully discharged battery.

Although the MCP charging method is the most popular of the conventional lead–acid battery charging systems, it has several inherent disadvantages. Some of these disadvantages result from the fact that, in some lead–acid batteries, the gassing potential is lowered with battery age. Since it is not convenient to adjust the charge bus voltage to compensate for this change, aging batteries gas more profusely and progressively earlier in the charge. This results in not only less efficient charging but in shortened battery life.

Another disadvantage results from the manner in which the charging current is regulated by this charging method. The battery voltage approaches the charger bus voltage asymptotically. The result is that, as the battery approaches full charge, more time is required to apply progressively less charge to the battery. A 100% charge is virtually impossible by this method, or for any charging method which employs an exponentially decaying charging current profile (see Fig. 2).

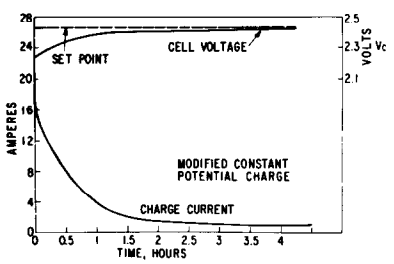

Fig. 2. Charging current and voltage profile, modified constant potential charge method.

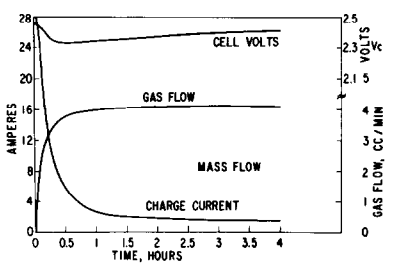

Fig. 3. Charging current, voltage, and mass flow profiles; mass flow charge.

The mass flow (MF) controlled charge is characterized by a charging current which is inversely proportional to the flow rate of gas from either or both electrodes of a charging battery. At the beginning of charge, when no gas is being evolved from either electrode, the charging current is at its preset maximum, 24 A for this study. As gas is evolved, the charging current is diminished so that the gas flow rate does not exceed the set point. Since the

charge acceptance of the battery diminishes with charge, progressively less charging current is required to maintain the preset gas flow. Finally, at the end of charge all of the charging current results in gassing. By definition, the battery is 100% charged and is being maintained in the charged state by an overcharge of 0.24 A, all of which results in the electrolysis of water (see Fig. 3). Based on a theoretical 100% gassing of 11.2 cm^3/min/cell/A, this corresponds to a gas flow of $11.2 \times 0.24 = 2.688$ cm^3/min/cell.

While this charging method is not controlled directly by a voltage difference as in the case of the MCP method, and is, therefore, not immediately sensitive to battery age, it does require the battery to be sealed. Further, it requires a gas flowmeter with a voltage output, and some means for employing this voltage output in controlling the output of a charging power supply. A tapering charging current, similar to that realized in the MCP charging, also results in progressively longer times to charge active electrode material as the battery approaches full charge. This is inevitable where extremely high-efficiency charging is desired by a charging method which utilizes a tapering current profile which approaches exponential form.

The gas pressure (GP) controlled charge is characterized by a charging current that decays in direct ratio to the amount of evolved gas necessary to maintain a preselected differential gas pressure within the battery container. Since this system allows gas to escape from the battery container through a small controlled orifice, it is also controlled by gas flow. Unlike the MF charge control method, control does not begin until the preselected differential pressure is reached. This results in a charging current profile which begins as a constant current of 24 A and remains at 24 A until the set point 0.4 lb/in^2 (gauge) is reached. At this point, the charging current begins to diminish such that the differential pressure is maintained. This calibrated differential pressure corresponds to the same flow of gas from the battery as for the MF-controlled charging method. Shown in Fig. 4 are the current, voltage, and pressure profiles used for this charging method.

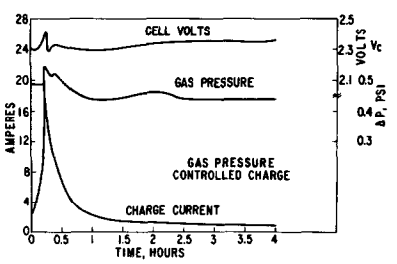

Fig. 4. Charging current, voltage, and differential pressure profiles; gas pressure charge method.

This method requires a pressure transducer with a voltage readout and a means for using that readout to control the output of the charging circuit power supply.

Since both gas-controlled charge methods described in this report require sealed batteries, they present potential hazards resulting from runaway charging. In practice, thermal overload or overvoltage devices can be utilized in the prevention of runaway during charging. Life-testing control circuits, used for this program, included overvoltage control devices which worked well. Other potential problems associated with this type of charge control can be solved with present state-of-the-art electronic and other controls.

Description of Batteries

All of the data for this program were obtained on two types of commercially available lead–acid batteries, both of which have cast lead–antimony grids. Each of the battery types contained three cells and was rated at 12 Ah. The chief differences between the two battery types were the number of plates per cell and the discharge rates used by the manufacturers for the rating of the batteries. The two battery types, type A and type B are described as follows:

	Battery A	Battery B
Weight/cell (g)	570	575
Volume/cell (cm^3)	326	374
Discharge rate for nominal capacity (h)	10	20
Number of positive plates/cell	8	4
Number of negative plates/cell	9	5
Positive plate thickness (cm)	0.165	0.165
Negative plate thickness (cm)	0.140	0.127
Positive plate area per plate two sides (cm^2)	58	120
Negative plate area per plate two sides (cm^2)	58	120
Positive plate volume (cm^3)	38 (8 plates)	40 (4 plates)
Negative plate volume (cm^3)	36 (9 plates)	38 (5 plates)
Separator volume (cm^3):		
microporous rubber	48	23
highly porous glass mat	37	—
highly porous polymers	—	85
Electrolyte volume (cm^3):		
below plates	10	7
separator and electrodes	101	118
between plates	22	9
above plates	20	0
Total electrolyte volume	153	134

Qualitative chemical analysis showed tin as an impurity in the antimonial grid of both types of batteries. This was followed by quantitative X-ray emission analysis of the grids of both type A and type B batteries which gave the following results:

	Wt. %	
	Antimony	Tin
Battery A:		
positive grid	3.8	0.07
negative grid	4.1	0.08
battery post	2.5	0.04
Battery B:		
positive grid	6.1	0.04
negative grid	6.5	0.05
battery post	3.9	0.03

Experimental

Data logging

Battery characterization consisted of carefully monitoring the following seven parameters as a function of time during charging: battery voltage, V_b; positive electrode to Hg/Hg_2SO_4, V^+; negative electrode to Hg/Hg_2SO_4, V^-; charging current (A), I_t; gas flow (cm^3/min), F_t; oxygen in gas (%), O_2; temperature (°C), T.

The following were then calculated from the measured data: cell voltage, V_c; oxygen flow (cm^3/min), F_o; hydrogen flow (cm^3/min), F_h; charging current, positive electrode, I^+; charging current, negative electrode, I^-; total amp-hour charge, Aht; Ah charge, positive electrode, Ah+; Ah charge, negative electrode, Ah—; Total watt-hour charge, Wht; Wh charge, positive electrode, Wh+; Wh charge, negative electrode, Wh—.

From these computer calculated data, the following performance indicators were obtained from the batteries' discharge capacity (Ah dis):

Total amp-hour efficiency (%)	%Ah (Ah dis/Aht)
Amp-hour efficiency, positive electrode (%)	%Ah+ (Ah+/Aht)
Amp-hour efficiency, negative electrode (%)	%Ah— (Ah—/Aht)
Total watt-hour efficiency (%)	%Wh (Wh dis/Wht)
Watt-hour efficiency, positive electrode (%)	%Wh+ (Wh+/Wht)
Watt-hour efficiency, negative electrode (%)	%Wh— (Wh—/Wht)
Positive charge retention (%)	%CR+ (Ah dis/Ah+)
Negative charge retention (%)	%CR— (Ah dis/Ah—)

The above data logging procedure was followed while each of the batteries was being charged at constant current, 1.2 A, and while each of the batteries was being charged under one of the three charging modes under investigation.

Results

Three constant current charge characterizations and three characterizations under one of the charging modes being investigated were run for each battery during its life as measured by the life-test cycling. After preconditioning each of the six batteries by constant current charge and discharge cycling at the C/10 rate, the following sequential steps were used for characterizing and life-testing of the batteries: (1) characterization using a C/10 charging rate for 12 hours followed by a C/10 discharge to 1.75 V/cell; (2) characterization using one of the three charging modes under investigation followed by a C/10 discharge to 1.75 V/cell; (3) repetitive charge–discharge cycling (life-testing) using one of the charging methods under investigation and discharges at the C/10 discharge rate to 1.75 V/cell.

In addition to characterization measurements of new batteries, characterization measurements were repeated when the battery under investigation had degraded to 75% of its initial discharge capacity, and finally when the battery had degraded to 50% of its initial discharge capacity* as determined from the life-testing portion of the program. For this program, a battery which had degraded to 50% of its initial stabilized discharge capacity was considered spent.

Six batteries were evaluated for this program: three type A batteries and three type B batteries. For purposes of identification, a code was used to identify each charging mode, battery type, type of characterization, and characterization number. The code consists of three groups of letters followed by a digit, for example: MCP-A-CC-1. The first group of letters identifies this as a battery normally cycled by the MCP method. The second letter identifies the battery (type A). The third group of letters indicates the characterization method for a particular characterization — Constant Current (CC). The digit identifies a characterization number (1). A total of six characterizations was planned for each battery: three characterizations at constant current and three characterizations at one of the charging modes. Codings for these six batteries are:

MCP-A MCP-B	Modified constant potential
MF-A MF-B	Mass flow

*In two cases (batteries MF-B and GP-B) this 50% criterion was applied to the maximum attained capacity rather than the initial capacity.

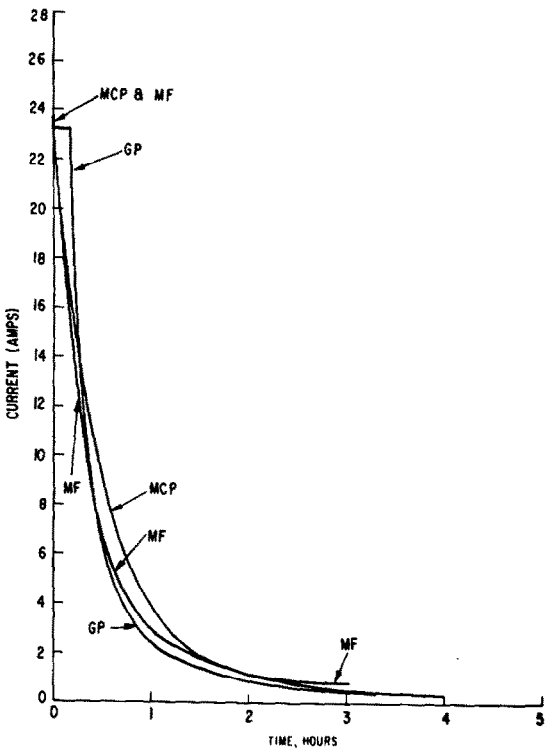

Fig. 5. Current profile for the three different charging modes.

GP-A
GP-B Gas pressure

As a distinction between the characterizations of the three different charging modes, Fig. 5 presents the charge current as a function of time for the three methods.

Computerized manipulation of characterization data

From the above discussion of battery and characterization coding, it is apparent that in addition to the life-test data, 36 blocks of data were generated during the six characterization of six batteries.

In this report, only summary tables of the computer-generated data are shown. Tables 1 and 2 are summaries of the Ah and Wh efficiencies as well as charge acceptance and discharge recovery calculated from the computer readout sheets.

Life-test data were obtained by continuous automatic cycling. In all cases, constant current discharges of 1.2 A were terminated at 1.75 V per cell. The actual cycle life-test data are given in Table 3.

TABLE 1

Summary data-characteristics of batteries with constant current mode characteristics

Battery No.	Characterization No.	Mode	No. of Cycles	Ah			Wh			% charge acceptance**		Ah recovery (%) discharge***	
				Charge	Dis.	Eff.	Charge	Dis.*	Eff.	Pos.	Neg.	Pos.	Neg.
MCP-A	1	CC	1	14.4	12.0	83	33.8	23.3	69	—	—	—	—
	2	CC	98	14.9	12.5	84	34.4	24.4	71	73	77	115	109
	3	CC	131	14.1	8.6	61	31.2	16.8	54	90	93	68	65
MF-A	1	CC	1	14.4	12.3	85	32.3	24.0	74	97	91	88	93
	2	CC	—	—	—	—	—	—	—	—	—	—	—
	3	CC	—	—	—	—	—	—	—	—	—	—	—
GP-A	1	CC	1	15.0	11.2	75	33.1	21.8	66	83	85	89	87
	2	CC	124	15.5	10.1	65	36.7	19.8	54	54	63	121	103
	3	CC	177	19.1	11.1	58	44.7	21.7	48	54	56	107	103
MCP-B	1	CC	2	14.6	11.1	76	33.3	21.7	65	89	82	85	93
	2	CC	120	14.6	9.66	66	33.0	18.8	57	85	89	77	74
	3	CC	325	10.2	6.54	64	22.6	12.8	57	93	93	68	68
MF-B	1	CC	2	14.5	11.4	79	32.1	22.2	69	90	84	87	94
	2	CC	135	13.8	10.3	75	31.6	20.1	64	57	67	99	111
	3	CC	190	13.8	6.23	45	31.7	12.1	38	61	66	67	68
GP-B	1	CC	2	14.4	11.5	80	63.8	22.4	35	93	93	84	84
	2	CC	122	14.2	4.75	33	32.2	9.4	29	78	73	43	46
	3	CC	174	13.8	4.97	36	30.9	9.7	31	73	81	49	45

*Average voltage during discharge = 1.95 V.

**$Ah_{\pm}/Aht.$

***$Ah_{dis}/Ah_{\pm}$.

TABLE 2

Summary data-characterizations at modified constant potential, mass flow, and gas pressure controlled charges

Battery No.	Characterization No.	Mode	No. of Cycles	Ah			Wh			% charge acceptance**		Ah recovery (%) discharge***	
				Charge	Dis.	Eff.	Charge	Dis *	Eff.	Pos.	Neg.	Pos.	Neg.
MCP-A	1	MCP	2	15.0	12.5	83	36.7	24.2	66	—	—	—	—
	2	MCP	97	13.6	10.1	74	32.5	20.3	61	73	75	102	100
	3	MCP	130	14.0	9.4	67	32.3	18.3	57	58	91	115	74
MF-A	1	MF	2	12.3	10.8	88	29.1	21.0	72	97	91	88	93
	2	MF	—	—	—	—	—	—	—	—	—	—	—
	3	MF	—	—	—	—	—	—	—	—	—	—	—
GP-A	1	GP	2	12.9	11.9	92	31.0	23.1	75	81	81	113	113
	2	GP	123	7.1	6.3	89	15.9	12.3	77	84	87	105	102
	3	GP	176	11.7	10.6	91	27.0	20.6	76	88	89	103	101
MCP-B	1	MCP	1	16.2	11.6	71	40.7	22.3	55	76	72	93	99
	2	MCP	119	10.4	8.3	80	24.0	16.2	67	95	97	84	82
	3	MCP	324	20.0	8.7	44	48.0	17.0	35	70	58	62	75
MF-B	1	MF	1	13.2	10.6	80	31.4	20.6	66	98	99	82	82
	2	MF	134	9.5	8.9	94	22.5	18.5	82	89	89	106	105
	3	MF	189	6.8	5.4	79	16.2	10.5	65	84	84	94	94
GP-B	1	GP	1	13.2	9.8	74	30.9	19.1	62	93	93	80	81
	2	GP	121	11.9	4.0	30	27.7	7.7	28	79	81	42	41
	3	GP	173	10.4	5.0	48	24.6	9.8	40	78	76	61	63

*Average voltage during discharge 1.95 V.

**$Ah_{\pm}/Aht$.

***$Ah_{dis}/Ah-$.

TABLE 3
Life tests

Cycle No.	MCP-A Disch. (Ah)	MF-A Disch. (Ah)	GP-A Disch. (Ah)	MCP-B Disch. (Ah)	MF-B Disch. (Ah)	GP-B Disch. (Ah)
1	12.5	10.8	10.8	11.6	7.6	9.0
2	10.8	9.9	10.1	11.4	7.5	8.3
3	11.4	12.1	10.1	11.4	4.7	7.7
4	10.9	12.4	11.9	11.6	7.0	8.1
5	10.7	11.0	11.0	11.4	7.0	7.7
6	10.6	11.0	11.0	11.4	7.1	7.6
7	10.7	10.7	10.4	11.0	6.7	7.4
8	10.9	10.1	9.6	10.4	6.3	7.3
9	10.9	11.1	9.2	11.1	6.0	7.4
10	10.4	11.1	8.6	10.9	5.8	7.2
(Avg. 1 - 10)	(11.0)	(11.0)	(10.3)	(11.2)	(6.6)	(7.8)
20	10.4	11.1	11.2	11.7	4.8	6.6
30	10.6	10.9	10.3	9.6	4.8	6.6
40	10.7	10.7	8.8	11.2	8.1	5.0
50	10.9	11.0	7.6	8.6	8.0	3.2
60	10.1	10.7	8.6	8.9	9.4	—
70	9.8	10.0	8.5	7.8	9.3	—
80	9.8	9.8	8.6	8.9	9.2	8.4
90	10.2	9.5	7.0	10.8	7.3	4.8
100	11.8	10.2	7.6	9.1	9.2	6.0
110	10.2	9.7	7.0	10.0	9.1	3.5
111		9.5				
120	9.6	———	6.2	9.7	9.3	4.4
129	5.7	(Failed)				
130	———		6.6	9.2	8.6	8.0
140			6.1	6.7	8.9	8.0
150			5.8	9.3	7.7	8.8
160			5.5	9.3	6.1	5.3
170			5.7	8.7	5.2	4.7
172						4.4
175			5.5			———
180			———	8.8	4.7	
188					4.8	
190				8.9	———	
200				7.8		
210				8.2		
220				7.9		
230				7.6		
240				8.5		
250				7.3		
260				7.1		
270				6.8		
280				6.4		
290				8.0		
300				8.8		
310				7.9		
320				6.8		
325				6.5		
				———		

Discussion

Cycle life

The longest-lived battery was MCP-B with 325 cycles. In this respect the MCP mode was best. Likewise, efficiencies in terms of Ah and Wh obtained in discharge relative to the previous charge were about the same for the MCP mode and the two gas-controlled modes. However, each comparison has its own qualification, so that the overall picture is not clear-cut. For example, with respect to the long life of battery MCP-B, this particular battery and charging mode also entailed more undesirable gas evolution than any of the other batteries or methods.

It was also observed that prolonged overcharges at an end of charge rate less than that normally employed result in a capacity recovery for the immediately following discharge. A return to the originally selected end-of-charge current results in an immediate drop in discharge capacity to that observed before the end of discharge current perturbation. This observation shows that the active material is not sloughed off the battery plates or permanently buried under passivated electrode material. It may be due to some other change in the physical structure of the battery plates.

Charging efficiencies

Columns 7 and 10 of Tables 1 and 2 show that the Ah and Wh efficiencies are more determined by the charging mode than by the cycle number in the life of a battery, except insofar as the cycle number reflects a relatively abrupt deterioration of the battery. Thus, the efficiencies in the MCP method decrease slightly during the cycle life of batteries MCP-A and MCP-B. This corresponds to a larger fraction of the current going into gas evolution which can only be compensated for by an increase in the end-of-charge current. Conversely, in gas control, efficiencies should have been independent of the tendency towards gas evolution because a fixed gassing rate controls the charge current. This does not allow undue gassing. Instead, less useful charging takes place. This could be the source of undercharging in the series MF-B and GP-B.

The most obvious weakness in all batteries was the decrease of hydrogen overvoltage at the negative plates which caused the increased gassing and greater inefficiencies. This is reflected in all three different charging modes. However, inspection of Tables 1 and 2 will show that in terms of Ah efficiency all batteries except MF-A and GP-B maintained reasonable efficiencies throughout cycle life. MF-A failed because of instrumental breakdown, so that GP-B was the only poorly performing battery of the six batteries tested.

Speed of charge

Gas-controlled charges, as they have been applied for this program, have focused on charging efficiency. Where charge acceptance is high, such as at the beginning of charge of a previously completely discharged battery,

rate of charging and efficiency of charging are high. As the battery becomes partly charged, its charge acceptance decreases but its charging efficiency remains high by the gas-control methods. This results in a prolonged time of charge at high efficiency because of the diminishingly small amounts of uncharged active material. These data show that, near the beginning of charge, the GP method is fastest in terms of charge returned to the battery. However, as the charge continues, differences between the GP, MF and MCP charges, in terms of capacity restored, become less apparent. By any of the three charging methods, and particularly the gas-controlled methods adjusted for very efficient charging, 100% charges of previously discharged capacity are difficult and become more difficult if high charging efficiency is required.

Charge acceptance and Ah recovery on discharge

These parameters, given in the last four columns of Tables 1 and 2, reflect the efficiency of charging individual electrodes and their ability to deliver that charge on the subsequent discharge. Because of the larger amount of gassing in the MCP mode, the charge acceptance in this mode should have been somewhat lower than for the other methods. This was observed in characterization MCP-B-3. Recovery was almost uniformly good except at the end of cycle life in the third characterization and for the second characterization of battery GP-B.

MCP charging

Both batteries MCP-A and MCP-B deteriorated because of usual causes of failure, namely the corrosion of the positive grid, shedding, and bridging of the positive plate materials. In addition, lowering of the hydrogen overpotential at the negative electrode in batteries with grids containing antimony causes earlier hydrogen gassing, which in turn is reflected in lower charge acceptance. Worsening performance may be due to gassing from the negative plate; the actual battery failure can be attributed to the positive plate. For example, in battery MCP-A, this is consistent with the concurrent decrease of the negative plate potential to lower values during the course of cycle life; *viz.*, 1.41 to 1.22 to 1.14 V *vs.* Hg/Hg_2SO_4 in the three characterizations. Thus, the stoichiometric evolution of hydrogen and oxygen was maintained although the positive material deteriorated to a greater extent than the negative. There was appreciable charge acceptance and good charge retention, limiting gas evolution, in the second characterization, but poor performance in the final characterization.

Battery MCP-B similarly showed a decrease in hydrogen overpotential which required frequent replenishment of water lost by excessive gassing. However, given the handicap, the longest cycle life of all batteries tested was achieved by battery MCP-B.

This also required having the charging cycle terminated at relatively high currents in the later stages of cycling (1.20 to 1.60 A, equivalent to the C/10 to C/7.5 rates).

Gas-controlled charge (MF and GP)

Since these are gas-flow-controlled charges, gassing at lowered negative potential due to antimonial contamination resulted in a concomitant reduction in the charging current. The net effect was a virtually unchanged charging efficiency but longer time on charge as a given battery containing Pb/Sb grids ages. This effect was noted particularly on life-test. Batteries cycled by either the MF or the GP methods required progressively longer charging times as they aged. For this reason, the end of charge current cutoff was raised resulting in a shorter time on charge.

Previous work had shown the advantages of gas-controlled methods. MF and GP were selected for further study with respect to life-testing as the most promising methods. However, the life-test data of this study are not sufficiently conclusive to confirm the expectation. Only in the case of GP-A was there found a superior charging performance for gas control. As pointed out previously, the longest cycle life was obtained with MCP-B. The advantage of gas control lies in limiting the loss of water from the electrolyte, but this is achieved at the cost of undercharging. An occasional deliberate overcharge of the battery shows that the capacity is still available, but it is not completely used in either of the two gas-control modes.

Failure analysis

All batteries were subjected to failure analysis. There was less positive grid corrosion and shedding of active material in type A batteries than in type B batteries. GP-B failed because of bridging of plates by shedded positive material. Corrosion of positive grids in type B batteries followed the order MCP > GP > MF, from worst to least corrosion.

Batteries with type A vs. *type B design*

The two types of batteries are described above. Their designs were different. Yet, they are very similar in terms of weight and geometry; *i.e.*, weight and volume of components, and most importantly, as far as the volume, thickness, and surface area of the plates are concerned as well as the amounts of acid and its density.

One major difference was the tight wrapping of type B cell packs in a woven polymeric cloth. This had the advantage of preventing the loosening and shedding of active material, but had also the disadvantage of a more compressed construction causing whatever dendrite or spalling takes place to bridge the plates for a short. In fact, that was observed in at least one case.

Another difference is the composition of the antimonial grid alloy. The type A battery had only about 4% Sb in both positive and negative grids compared to more than 6% for the type B battery. This may not be directly related to cycle life or battery performance since antimony caused gassing in both cases. However, inspection of the batteries showed that the positive grids of type A were less corroded and this may be related to the lower Sb content of type A grids.

Undercharging occurred in gas-controlled charging modes. It was a more serious problem for type B than for type A batteries. The effect was pronounced as shown in Table 3. Although the cause of this is not known, it may be traced to the higher antimony content of the type B batteries which could have resulted in higher gassing rates.

Combination of charging mode with battery type

Inspection of Tables 1 and 2 does not show any outstanding difference in the cycle life and performance of the various possible combinations of charging modes and batteries.

Longer life time of MCP-B was obtained. However, this battery exhibited more gassing and experienced more positive grid corrosion than in the corresponding gas control methods. Conversely, MCP-A had a slightly shorter cycle life than GP-A and presumably that of MF-A, had it not failed for instrumental reasons.

It appears, therefore, that the results of this study do not discriminate strongly between the different charging modes for the kind of batteries and heavy-duty cycling regimes used in the present work. Gas control requires more elaborate electronic circuitry. Maintenance of precise and sensitive mechanical conditions of gas flow is also necessary. The former presents no problems because there is a very substantial electronic technology, either with operational amplifiers or with miniaturized circuits, which can handle the electrical part of the charging controls. The mechanical control of the gas flow may, however, be more difficult to control in a totally automated system over the lifetime of a battery that is intended to last for many years. Conversely, the MCP method is much simpler in principle; but as detailed above, this method too has its drawbacks. The data collected during the characterizations of the batteries used for this program illustrate the possibility for quick, efficient charging by the gas-controlled methods and the MCP method where the initial charging currents are at the 2 C rates. A convenient method for evaluating a charging system in terms of rapid charging is to measure the percentage of capacity restored in a short time on charge, *e.g.* 0.5 h. For this program, the characterization data were compared with the discharge capacity for the discharge immediately preceding the characterization. For new batteries charged by the three methods used for this program, the percentage of previously discharged capacity restored in 0.5 h was as follows: MF, 63%; MCP, 69%; GP, 90%. In general, as the batteries aged, they recharged at a somewhat diminished but still appreciable rate. This occurred because of reduced charge acceptance; progressively more charging current resulted in gassing.

The above percentage recovery data were obtained on batteries subjected to complete discharges. Other parameters such as realistic duty cycle, operating temperature, and ultimate battery life need to be considered before definite conclusions could be reached concerning the effectiveness of a given charging method for quick charging of electric vehicles.

Conclusions

(1) The three charging modes, although very different in principle, gave equivalent performances in combination with lead–acid batteries having antimonial grids.

(2) The MCP method is preferred for simplicity of equipment and operation. However, more corrosion, more gassing, and the consequently more frequent maintenance were observed and required.

(3) The gas-controlled methods are relatively maintenance-free. Little water was lost from the batteries by electrolysis, but undercharging was a problem.

(4) In all cases, more sensitive and uniform control was achieved with gas-controlled charging throughout the cycle life of both types of batteries.

(5) Charging speed is dependent upon the charging mode mainly in the beginning of charge. As charging progresses, differences in charging rates for the different charging modes become less pronounced.

(6) It is difficult to charge 100% previously discharged capacity, especially if high charging efficiency is required.

(7) Where obvious failure occurred, it was caused by the bridging of positive active material at the edges and at the bottom of the cell pack. Some positive grid corrosion was also noted.

Acknowledgement

This work was sponsored and partially financially supported by the International Lead Zinc Research Organization, Project LE205. The contributions of D. F. Taylor in initiating this program are gratefully acknowledged.